THE PECULIAR OPTICAL SPECTRUM OF 4C+22.25: IMPRINT OF A MASSIVE BLACK HOLE BINARY?

R. Decarli[1], M. Dotti[2], C. Montuori[3], T. Liimets[4,5], and A. Ederoclite[6,7]
[1] Max-Planck Institut für Astronomie, Königstuhl 17, D-69117 Heidelberg, Germany; decarli@mpia.de
[2] Max-Planck-Institut für Astrophysik, Karl-Schwarzschild-Str. 1, D-85748 Garching, Germany; mdotti@mpa-garching.mpg.de
[3] Dipartimento di Fisica e Matematica, Università dell'Insubria, via Valleggio 11, I-22100 Como, Italy
[4] Nordic Optical Telescope, Apartado 474, E-38700 Santa Cruz de La Palma, Santa Cruz de Tenerife, Spain
[5] Tartu Observatory, Tõravere 61602, Estonia
[6] Instituto de Astrofísica de Canarias, E-38200 La Laguna, Tenerife, Spain
[7] Departamento de Astrofísica, Universidad de La Laguna, E-38205 La Laguna, Tenerife, Spain
Received 2010 June 11; accepted 2010 July 19; published 2010 August 13

ABSTRACT

We report the discovery of peculiar features in the optical spectrum of 4C+22.25, a flat spectrum radio quasar at $z = 0.4183$ observed in the Sloan Digital Sky Survey and in a dedicated spectroscopic follow-up from the Nordic Optical Telescope. The Hβ and Hα lines show broad profiles (FWHM $\sim$ 12,000 km s^{-1}), faint fluxes, and extreme offsets ($\Delta v = 8700 \pm 1300$ km s^{-1}) with respect to the narrow emission lines. These features show no significant variation in a time lag of $\sim$3.1 yr (rest frame). We rule out possible interpretations based on the superposition of two sources or on recoiling black holes, and discuss the virtues and limitations of a massive black hole binary scenario.

Key words: quasars: individual (4C+22.25)

Online-only material: color figure

1. INTRODUCTION

4C+22.25 (R.A.: 10:00:21.8; decl.: +22:33:19 (J2000.0)) is a flat spectrum radio quasar at $z = 0.4183$, discovered through radio observations by Merkelijn et al. (1968). A first optical spectrum was collected by Schmidt (1974) who observed a flat continuum with no significant emission line, suggesting that the source is a BL Lac object. Haddad & Vanderriest (1991) re-observed the 4000–6000 Å range and detected a set of bright, marginally resolved narrow lines ([Ne v]$_{3346,3426}$; [Ne iii]$_{3869,3968}$; [O ii]$_{3727}$; Hγ, [O iii]$_{4363}$) at $z = 0.419$. The intensity ratios of these lines suggested that the source hosts a Seyfert-like narrow-line (NL) region. Nilsson et al. (2003) collected ground-based high-resolution images of 4C+22.25 as a part of a study of blazar host galaxies and showed that the host galaxy is well resolved. Its light profile follows a de Vaucouleurs law with scale radius $R_e = 3''.3 \pm 0''.2$ (18 ± 1 kpc) and apparent magnitude $m_R = 18.63 \pm 0.05$. Including a k-correction (0.7 mag assuming a typical Elliptical galaxy spectrum at $z = 0.419$), the inferred luminosity is $M_R = -23.9$.

A companion galaxy is located $\sim$6$''$ northwest of 4C+22.25 ($\sim$30 kpc at the redshift of the quasar). Haddad & Vanderriest (1991) reported the detection of the Ca ii (H) and G-band features in its spectrum, yielding $z = 0.416$, and suggested that a gravitational interaction with the quasar host galaxy may be occurring. Sloan Digital Sky Survey (SDSS) photometry also reveals the presence of 12 galaxies within a projected separation of 400 kpc and photometric redshift consistent with the one of 4C+22.25, suggesting that the source may be located in a relatively rich galactic environment.

In this Letter, we report the discovery of peculiar broad lines in the optical spectrum of 4C+22.25 that is publicly available from the SDSS (York et al. 2000) database. Very broad and rather faint Mg ii, Hβ, and Hα lines are observed, all showing a velocity blueshift of $\approx$8700 km s^{-1} with respect to the NLs.

Similar velocity offsets have been already observed in a handful of SDSS quasars: Komossa et al. (2008) reported a $\sim$2650 km s^{-1} shift between the main NL system and a second set of narrow and broad lines in SDSS J092712.65+294344.0 (hereafter J0927), which has been interpreted as the signature of a recoiling black hole (Komossa et al. 2008), of a massive black hole binary (BHB; Bogdanovic et al. 2009; Dotti et al. 2009) or the superposition of two objects (Heckman et al. 2009). Similarly, Shields et al. (2009) found a $\sim$3500 km s^{-1} shift between narrow and broad lines in the spectrum of SDSS J105041.35+345631.3 (hereafter J1050). Finally, Boroson & Lauer (2009) revealed the presence of a peculiar profile in the broad lines of SDSS J153636.22+044127.0, which could be due to a BHB (Boroson & Lauer 2009; Lauer & Boroson 2009), a superposition of quasars (Wrobel & Laor 2009; Decarli et al. 2009a), or an extreme double-peaked emitter (Tang & Grindlay 2009; Chornock et al. 2010). However, we show here that most of these interpretations are unsuitable for 4C+22.25.

The structure of this Letter is the following: in Section 2, we analyze the SDSS spectrum and present new observations collected at the Nordic Optical Telescope (NOT). In Section 3, we discuss possible models to interpret the peculiar features of this source. Conclusions are summarized in Section 4. Throughout the Letter, we will assume a standard cosmology with $H_0 = 70$ km s^{-1} Mpc^{-1}, $\Omega_m = 0.3$, and $\Omega_\Lambda = 0.7$.

2. THE SPECTROSCOPIC OBSERVATIONS

2.1. SDSS Spectrum

The SDSS spectrum of 4C+22.25 was collected on 2006 January 2 and was published in the SDSS Sixth Data Release (Adelman-McCarthy et al. 2008). SDSS spectra have $\lambda/\Delta\lambda \sim$ 2000 and cover the 3800–9000 Å range. Uncertainties on wavelength calibration amount to 0.05 Å, while flux calibration formal errors account to 5%. The signal-to-noise ratio per pixel at 6400 Å is 21.

Figure 1 shows the SDSS spectrum (top panel) and the identification of main emission lines (bottom panel). Emission lines were fitted with a double-Gaussian profile, following Decarli et al. (2008). Relevant information is provided in Table 1. Typical uncertainties in the line FWHM are around
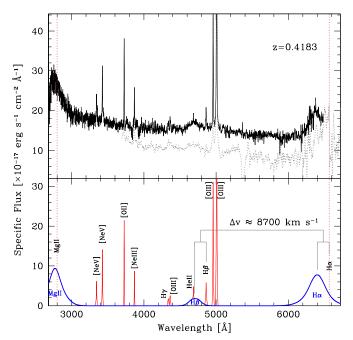
Figure 1. Top panel: SDSS (solid line) and NOT (dotted line) spectra of 4C+22.25, shifted to the rest frame assuming $z = 0.4183$. The NOT spectrum is shifted downward for the sake of clarity. No significant difference in the two spectra is reported. Bottom panel: the fitted components. Thick lines mark the broad lines, thin lines mark the narrow features. The two vertical dotted lines show the rest-frame wavelengths of Mg II and Hα. The Mg II line model is poorly constrained since the line lays are at the edge of the SDSS coverage. The velocity shift between the broad and the narrow line systems is clearly apparent.

(A color version of this figure is available in the online journal.)

10%. NL peak wavelengths have uncertainties of 10 to few hundred km s^{-1} depending on the line flux (see Table 1). The broad line peak wavelengths are poorly constrained: for Hβ and Hα, we estimate recessional velocity uncertainties of 1900 and 1700 km s^{-1}, respectively. The NLs are marginally resolved. Their mean redshift is $\langle z \rangle = 0.4183$. The [O III]/[O II], [O III]/Hβ, and [Ne V]/[Ne III] flux ratios confirm the presence of Seyfert-like ionization conditions in the NL region (see Figure 2 and Heckman 1980; Haddad & Vanderriest 1991).

For the first time, we report the detection of broad lines in 4C+22.25. The Hα, Hβ, and Mg II lines are clearly visible, while broad components of other Balmer lines and the iron multiplets are too faint to be detected. Both Hα and Hβ are very broad (FWHM $\sim$ 12,000 km s^{-1}, i.e., larger than 96% of the quasars in the huge, SDSS-based data set by Shen et al. 2010) and faint with respect to, e.g., the narrow [O III] lines (see Figure 2; only 1.1% of the quasars in Shen et al. (2010) have larger [O III]/Hβ (broad) values). The most striking property of these lines is that they show enormous blueshifts (8700 $\pm$ 1300 km s^{-1}) with respect to the NL system. Similar properties (in terms of fluxes, line width, and shift) are reported also for the Mg II line, but since the peak is close to the range covered by the SDSS spectrum, the line characterization is not feasible with the available data. We use the line width and luminosity of broad Hβ to compute the mass of the active black hole, following Vestergaard & Peterson (2006): $M_{\rm BH} = 1 \times 10^9 \, M_\odot$. Assuming the bolometric correction factor by Richards et al. (2006) for the continuum luminosity at 5100 Å, this yields $L/L_{\rm Edd} = 0.035$.

Few absorption features are also tentatively reported, namely, the Mg II doublet, the Ca (H) and (K), and the NaD line, at a redshift consistent with the narrow emission lines.

Table 1
Summary of the Main Emission Lines as Observed in the SDSS and NOT Spectra of 4C+22.25

Line	$\lambda_{\rm obs}$ (Å)	z	Δv (km s^{-1})	FWHM (km s^{-1})	$\log L_{\rm line}$ (erg s^{-1})
(1)	(2)	(3)	(4)	(5)	(6)
SDSS spectrum					
[Ne V]	4745.8	0.4180	-60 ± 720	580	41.60
[Ne V]	4860.2	0.4183	-10 ± 120	560	41.87
[O II]	5288.2	0.4183	$+10 \pm 50$	490	41.96
[Ne III]	5488.9	0.4184	$+20 \pm 160$	410	41.53
Hγ(n)	6155.4	0.4178	-120 ± 600	1100	41.20
[O III]	6192.3	0.4188	$+110 \pm 500$	910	41.36
He II	6647.4	0.4183	-10 ± 300	280	41.08
Hβ(b)	6679.6	0.3736	-9700 ± 1900	12000	42.34
Hβ(n)	6897.4	0.4184	$+30 \pm 130$	570	41.68
[O III]	7035.2	0.4183	0 ± 30	430	42.25
[O III]	7103.0	0.4183	-8 ± 11	410	42.73
Hα(b)	9078.8	0.3830	-8000 ± 1700	12700	43.18
NOT spectrum					
Hβ(b)	6681.6	0.3740	-9400 ± 1600	13000	42.32
[O III]	7104.2	0.4185	$+50 \pm 30$	770	42.74

Notes. Column 1: line identification. When both broad and narrow components are available, they are marked with "b" and "n," respectively. Column 2: observed peak wavelength. Column 3: redshift corresponding to the observed peak wavelength. Column 4: velocity difference with respect to the mean redshift of the NL system, $\langle z \rangle = 0.4183$. Negative values correspond to blueshifts. Column 5: full width at half-maximum of the fitted lines. Note that no correction for spectral resolution is applied here. Column 6: line luminosity.

2.2. NOT Spectrum

We re-observed 4C+22.25 using the Andalucia Faint Object Spectrograph and Camera (ALFOSC) mounted on the 2.56 m NOT on 2010 June 2, i.e., 1612 days after the acquisition of the SDSS spectrum (1137 days in the rest frame of the source). Long-slit spectroscopy configuration was adopted. Grism 5 yields a spectral resolution $\lambda/\Delta\lambda \approx 410$ (1″.0 slit) in the spectral range 5500–10000 Å. The total integration time (45 minutes) was split into three exposures to allow an easy cleaning of cosmic rays. Standard IRAF tools were used to reduce data. Wavelength calibration was performed using Th–Ar arc spectra, and cross-checked using the sky emission lines in the science spectra. Wavelength residual rms is 1.3 Å. Flux calibration was achieved observing a spectrophotometric standard star. Galactic extinction was accounted for according to Schlegel et al. (1998), assuming $R_V = 3.1$. The final spectrum is shown in Figure 1 (top panel). Its signal-to-noise ratio per pixel at 6400 Å is 23. The NOT spectrum is in excellent agreement with the SDSS observation both in terms of fluxes and peak wavelengths of the observed features (see Table 1). Since the SDSS spectrum has a better global quality, we will refer to velocities and fluxes derived from the SDSS data in the following analysis.

3. DISCUSSION

3.1. What 4C+22.25 Cannot Be

A simple explanation of the two redshift systems observed in 4C+22.25 would be that the broad and narrow emission lines belong to two different objects, superimposed along the line of sight. This scenario is disfavored by the lack of narrow emission lines at the redshift of the broad line system (see also Boroson & Lauer 2009). We estimate that an NL as faint as 3.6×10^{40}
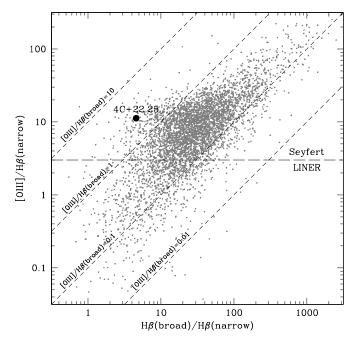
Figure 2. [O III]/Hβ(narrow) flux ratio plotted as a function of the ratio between broad and narrow Hβ components. The horizontal line marks the separation between Seyfert and LINER ionization conditions (see Heckman 1980). Diagonal lines show the loci of various [O III]/Hβ(broad) flux ratios. The big dot marks the position of 4C+22.25. For reference, we plot with small gray dots the flux ratios of the 18,101 quasars from the compilation by Shen et al. (2010) for which the three lines were detected. 4C+22.25 shows strong [O III] and very faint broad Hβ as compared to the average quasar population.

erg s^{-1} would be detected at 1σ with respect to the noise of the SDSS spectrum. This limit corresponds to 0.017× the flux of the broad component of Hβ. From Figure 2, it is apparent that the number of quasars with [O III]/Hβ(broad)<0.017 is negligible.

Moreover, in order to get both the sources within the fiber aperture of the SDSS, their separation should be <1″.5, yielding a solid angle < 5.5 × 10^{-7} deg^2. The number density of active galactic nuclei (AGNs) at 0.35 < z < 0.45 (i.e., in a velocity space three times as large as the velocity offset observed in 4C+22.25) is ~0.37 deg^{-2} (Schneider et al. 2010). Hence, the probability of having a random superposition is ~2 × 10^{-7}, i.e., completely negligible if compared to the number of SDSS AGNs in this redshift bin (~3300). The probability of alignment of two AGNs substantially increases if they belong to a common physical structure, e.g., a cluster of galaxy. This scenario was proposed by Heckman et al. (2009) to interpret the two redshift systems observed in J0927, but subsequent observations revealed that no significant cluster is present (Decarli et al. 2009b). The "superposition in a cluster" argument cannot be applied to 4C+22.25, as the velocity difference between the two line systems is too high to be attributed to the potential well of a single physical structure (see the statistical analysis by Dotti & Ruszkowski 2010).

Another scenario suggested to explain the velocity shifts between narrow and broad lines observed in J0927 and J1050 is that the black hole in these quasars is recoiling, as a result of the coalescence of a BHB (Komossa et al. 2008; Shields et al. 2009). The maximum recoil achievable during BH coalescence is ≲4000 km s^{-1} (Baker et al. 2008; Herrmann et al. 2007; Campanelli et al. 2007; Schnittman & Buonanno 2007; Lousto

& Zlochower 2009; van Meter et al. 2010).[8] As a consequence, the recoiling scenario is ruled out for 4C+22.25.

3.2. What 4C+22.25 Might Be

A possible alternative is that 4C+22.25 hosts a binary black hole. In this picture the primary, more massive BH resides at the center of a circumbinary gaseous disk, located in the nuclear region of the host galaxy, while a secondary black hole orbits around it. Because of its motion, the secondary black hole simultaneously accretes and prevents the primary one from accreting. The velocity shift between narrow and broad lines is then due to the Keplerian velocity of the secondary black hole with respect to the barycenter of the binary (for more details, see, e.g., Bogdanovic et al. 2009; Dotti et al. 2009). Assuming circular orbits, the orbital period t would be

$$t = 2\pi \frac{GM_2(\sin\vartheta\cos\phi)^3}{q(1+q)^2(\Delta v)^3},   \quad (1)$$

where M_1 and M_2 are the mass of the primary and secondary black holes, respectively, $q = M_2/M_1$, ϑ is the inclination angle of the rotational axis with respect to the line of sight, and ϕ is the orbital phase (defined so that $\phi = 0$ at the orbital node maximizing the blueshift of the broad lines). Similarly, the separation a between the two black holes would be

$$a = \frac{GM_2(\sin\vartheta\cos\phi)^2}{q(1+q)(\Delta v)^2}.   \quad (2)$$

In order to characterize the properties of the BHB, we therefore need an estimate of M_1 and M_2, which are unknown. Following Decarli et al. (2010), we use the host luminosity to infer the expected mass of M_1, assuming $M_{BH}/M_{host} = 0.0015$ as observed in the Local Universe (e.g., Marconi & Hunt 2003). For an old host galaxy stellar population, we infer $M_1 = 2 \times 10^9 M_\odot$. Assuming $M_2 = 1 \times 10^9 M_\odot$, as derived in Section 2, we obtain separations of 0.04–0.08 pc and orbital periods of 15–35 years for $\vartheta = 45°$–90° and $\phi = 0$. On the other hand, the velocity shift observed in the SDSS and the NOT spectra is unchanged within the uncertainties (~2000 km s^{-1}). This implies that the period should be ≳30 yr.

Small but not negligible eccentricities are expected in very massive BHBs, driven by three-body interactions with stars. For $q \sim 1$ (as in the present case), the maximum expected eccentricity is 0.1–0.3, depending on the mass of the binary and the steepness of the radial distribution of stars in the host galaxy (see Sesana 2010). Such small eccentricities do not significantly change our estimates.[9]

We point out that, at these tiny separations, the broad-line region is expected to be perturbed. This would explain the faintness of the broad lines with respect to the narrow lines (see Figure 2). In this case, the Vestergaard & Peterson (2006) recipe used to estimate M_2 may not be valid. We therefore adopt a different rule-of-thumb approach to estimate M_2, namely, assuming that the quasar is accreting at 10% of its Eddington

---

[8] Note that hydrodynamical and/or purely relativistic effects can strongly suppress the kick magnitude (Schnittman 2004; Bogdanovic et al. 2007; Dotti et al. 2010; Volonteri et al. 2010; Kesden et al. 2010).

[9] Higher eccentricities, besides being disfavored by models, are also ruled out by the absence of a velocity shift in the two observations. In a very eccentric orbit, the secondary black hole spends most of its time close to the apocenter, where the velocity has to be larger than (or equal to) the velocity observed in the spectrum (Δv). This implies that the period of the eccentric binary would be much shorter, hence incompatible with the observational constraints.

luminosity. In this case, $M_2 \approx 3 \times 10^8\, M_\odot$, $a \approx 0.05$–0.1 pc, and $t \approx 20$–60 yr. We conclude that the BHB scenario is a viable one for 4C+22.25.

4. CONCLUSIONS

We present the discovery of extremely peculiar features in the optical spectrum of the flat spectrum radio quasar 4C+22.25. The NLs are very bright and reveal the presence of a Seyfert-like nucleus. Its broad lines are faint and flat (FWHM $\sim$ 12,000 km s^{-1}), and blueshifted with respect to the NL of 8700 ± 1300 km s^{-1}. This velocity offset between broad and narrow lines is so high that scenarios involving a superposition in a cluster or a recoiling black hole are ruled out at high confidence. The probability of a chance superposition of two AGNs on cosmological scales is so small that it disfavored, especially if coupled with the non-detection of any narrow emission line at the redshift of the broad line system. The massive BHB scenario holds for 4C+22.25, but the observation of the target in two different epochs separated by 3.1 yr (rest frame) allowed us to set strong constraints on the possible orbital configurations. New observations with a longer time lag will help clarifying if the binary model is correct or not. Moreover, observations at higher frequencies, e.g., in the X-rays, would help in constraining the mass and Eddington rate of the accreting black hole.

Whether 4C+22.25 is a lone object, or just an extreme case of a new subclass of AGNs, including J0927 and J1050, is not clear, and demands further investigation both from a theoretical and an observational point of view.

Facilities: NOT(ALFOSC), Sloan

REFERENCES

Adelman-McCarthy, J. K., et al. 2008, ApJS, 175, 297
Baker, J. G., Boggs, W. D., Centrella, J., Kelly, B. J., McWilliams, S. T., Miller, M. C., & van Meter, J. R. 2008, ApJ, 682, L29
Bogdanovic, T., Eracleous, M., & Sigurdsson, S. 2009, ApJ, 697, 288
Bogdanovic, T., Reynolds, C. S., & Miller, M. C. 2007, ApJ, 661, L147
Boroson, T. A., & Lauer, T. R. 2009, Nature, 458, 53
Campanelli, M., Lousto, C. O., Zlochower, Y., & Merritt, D. 2007, ApJ, 659, L5
Chornock, R., et al. 2010, ApJ, 709, L39
Decarli, R., Dotti, M., Falomo, R., Treves, A., Colpi, M., Kotilainen, J. K., Montuori, C., & Uslenghi, M. 2009a, ApJ, 703, L76
Decarli, R., Falomo, R., Treves, A., Labita, M., Kotilainen, J. K., & Scarpa, R. 2010, MNRAS, 402, 2453
Decarli, R., Labita, M., Treves, A., & Falomo, R. 2008, MNRAS, 387, 1237
Decarli, R., Reynolds, M. T., & Dotti, M. 2009b, MNRAS, 397, 458
Dotti, M., Montuori, C., Decarli, R., Volonteri, M., Colpi, M., & Haardt, F. 2009, MNRAS, 398, L73
Dotti, M., & Ruszkowski, M. 2010, ApJ, 713, L37
Dotti, M., Volonteri, M., Perego, A., Colpi, M., Ruszkowski, M., & Haardt, F. 2010, MNRAS, 402, 682
Haddad, B., & Vanderriest, C. 1991, A&A, 245, 423
Heckman, T. M. 1980, A&A, 87, 152
Heckman, T. M., Krolik, J. H., Moran, S. M., Schnittman, J., & Gezari, S. 2009, ApJ, 695, 363
Herrmann, F., Hinder, I., Shoemaker, D. M., Laguna, P., & Matzner, R. A. 2007, Phys. Rev. D, 76, 084032
Kesden, M., Sperhake, U., & Berti, E. 2010, ApJ, 715, 1006
Komossa, S., Zhou, H., & Lu, H. 2008, ApJ, 678, L81
Lauer, T. R., & Boroson, T. A. 2009, ApJ, 703, L930
Lousto, C. O., & Zlochower, Y. 2009, Phys. Rev. D, 79, 064018
Marconi, A., & Hunt, L. K. 2003, ApJ, 589, L21
Merkelijn, J. K., Shimmins, A. J., & Bolton, J. G. 1968, Aust. J. Phys., 21, 523
Nilsson, K., Pursimo, T., Heidt, J., Takalo, L. O., Sillanpää, A., & Brinkmann, W. 2003, A&A, 400, 95
Richards, G. T., et al. 2006, AJ, 131, 2766
Schlegel, D. J., Finkbeiner, D. P., & Davis, M. 1998, ApJ, 500, 525
Schmidt, M. 1974, ApJ, 193, 505
Schneider, D. P., et al. 2010, AJ, 139, 2360
Schnittman, J. D. 2004, Phys. Rev. D, 70, 124020
Schnittman, J. D., & Buonanno, A. 2007, ApJ, 662, L63
Sesana, A. 2010, ApJ, 719, 851
Shen, Y., et al. 2010, arXiv:1006.5178
Shields, G. A., et al. 2009, ApJ, 707, 936
Tang, S., & Grindlay, J. 2009, ApJ, 704, 1189
van Meter, J. R., Miller, M. C., Baker, J. G., Boggs, W. D., & Kelly, B. J. 2010, ApJ, 719, 1427
Vestergaard, M., & Peterson, B. M. 2006, ApJ, 641, 689
Volonteri, M., Gültekin, K., & Dotti, M. 2010, MNRAS, 404, 2143
Wrobel, J. M., & Laor, A. 2009, ApJ, 699, L22
York, D. G., et al. 2000, AJ, 120, 1579